Very Rapid Forest Cover Change in Sichuan Province, China: 40 Years of Change Using Images From Declassified Spy Satellites and Landsat

Dan-Xia Song, Chengquan Huang, Tao He, Min Feng, Ainong Li, *Member, IEEE*, Sike Li, Yong Pang, Hao Wu, Abdul Rashid Mohamed Shariff, and John R. Townshend

***Abstract*—Forests have significant impacts on the global carbon cycle, hydrological processes, and biodiversity. Driven by socioeconomic developments, forests experienced drastic changes since the mid-20th century in China. Although declassified spy satellite and other Earth observation satellite data offer remote sensing technologies for mapping these long-term changes, challenges remain unsolved for applications of large volumes of historical data. This study uses long-term satellite observations, including declassified satellite data in the 1960s and Landsat products since the 1970s to monitor the decadal changes. A semi-automated method was developed for the rapid registration of declassified images with reference to Landsat data. The method was applied to quantify the forest cover (FC) in Sichuan Province (excluding Chongqing), China. Combined with a Landsat-based FC change product, it revealed that the FC in Sichuan declined rapidly by 38% from the 1960s to 2005. The FC was estimated to be 45.19 $\pm$ 1.62% in the 1960s and 38.98 $\pm$ 2.06% in 1975, but it rapidly decreased to 28.91 $\pm$ 2.07% in 1990 and 27.87 $\pm$ 2.14% by 2005. Supplemented with the official statistics, the FC in Sichuan was reported to increase to 38.03% by 2018. Although differences between the remote sensing-based estimates and the statistics were observed, they highlight the challenges in reconstructing historical land use changes for carbon and other studies. The drastic loss of forests before 1990 and the stabilizing afterward reflects the changes in forest policies, which transitioned from serving timber products to forest conservations.**

***Index Terms*—Declassified spy satellite (DSS), forest cover change (FCC), image registration, landsat.**

I. Introduction

China has undergone frequent social and economic changes that has led to rapid economic development and increased consumption of natural resources since the 1940s. For decades, the forest sector has been playing a role in providing timber products and fuel-wood to support economic development and population growth. Therefore, vast areas of natural forests have been damaged [1], and forests in China have possibly experienced an areal reduction or quality degradation of habitats in the 1960s, as evidenced in some nature reserves [2]. Alarmed by the devastating floods in 1998, China launched the logging ban and two major conservation programs, such as the Natural Forest Conservation Program (NFCP) and the Grain to Green Program (GTGP), aimed at mitigating environmental degradation and conserving natural resources through afforestation activities [3]. Forest cover (FC) in China increased from 12.7% in 1976 to 20.36% in 2008, according to official forest surveys [4], [5]. Such efforts to increase forest and other vegetation types have also contributed to a greening trend over the global vegetated areas since the 2000s [6].

Sichuan Province comprises a major part of the Southwest forested region, accounting for 43.9% of the timber reserves in China [7] including a large area of the primary forest [8]. Forests in Sichuan are currently run by a mixed management system of state-run and collective-run forests. Forest disturbance is mainly driven by long-term, complex human activities, especially at low-altitude regions and the Sichuan Basin. Liu *et al.* [2] found that suitable habitat for the giant panda was reduced by approximately 5100 ha before the establishment of the Sichuan Wolong Nature Reserve in 1975 and further reduced by 13% (~7300 ha) from its establishment until 1997 [2]. With the great potential of forest resources, Sichuan has been selected as the pioneer region for several forestry programs such as the NFCP, GTGP, and Yangtze River Shelter Forest Program [3]. As a result, a spatially and temporally comprehensive estimation of the forest

Manuscript received July 6, 2021; revised August 26, 2021 and September 18, 2021; accepted October 6, 2021. Date of publication October 19, 2021; date of current version November 10, 2021. This work was supported in part by the Natural Science Foundation of China under Grants 41901300 and 42090012, in part by the Fundamental Research Funds for the Central Universities under Grant CCNU19TD002, and in part by the Department of Geographical Sciences, University of Maryland, College Park. *(Corresponding author: Dan-Xia Song).*

Dan-Xia Song and Hao Wu are with the College of Urban and Environmental Sciences, Central China Normal University, Wuhan 430079, China (e-mail: dxsong@mail.ccnu.edu.cn; haowu@mail.ccnu.edu.cn).

Chengquan Huang and John R. Townshend are with the Department of Geographical Sciences, University of Maryland, College Park, MD 20740 USA (e-mail: cqhuang@umd.edu; jtownshe@umd.edu).

Tao He is with the School of Remote Sensing and Information Engineering, Wuhan University, Wuhan 430079, China (e-mail: taohers@whu.edu.cn).

Min Feng is with the National Tibetan Plateau Data Center Key Laboratory of Tibetan Environmental Changes and Land Surface Processes, CAS Center for Excellence in Tibetan Plateau Earth Sciences and Institute of Tibetan Plateau Research, Chinese Academy of Sciences, Beijing 100101, China (e-mail: mfeng@itpcas.ac.cn).

Ainong Li is with the Institute of Mountain Hazards and Environment, Chinese Academy of Sciences, Chengdu 610041, China (e-mail: ainongli@imde.ac.cn).

Sike Li is with the School of Earth Atmosphere and Environment, Monash University, Clayton Campus, VIC 3800, Australia (e-mail: sike.li@monash.edu).

Yong Pang is with the Institute of Forest Resource Information Techniques, Chinese Academy of Forestry, Beijing 100091, China (e-mail: pangy@ifrit.ac.cn).

Abdul Rashid Mohamed Shariff is with the Department of Biological and Agricultural Engineering Faculty of Engineering, Universiti Putra Malaysia (UPM), Serdang 43400, Malaysia (e-mail: rashidpls@upm.edu.my).

Digital Object Identifier 10.1109/JSTARS.2021.3121260

TABLE I
GLOBAL FCC PRODUCTS AT LANDSAT OR SIMILAR RESOLUTION

Product name	Temporal coverage	Spatial resolution	Classification scheme	Accuracy	Forest definition
1. Global Forest Change [11]	Annual map (2000 ~ 2014)	30 m	Tree cover in 2000, forest cover loss and gain	UA = 87%, PA = 88% for forest loss	All trees height > 5m
2. GLCF-GFCC (i.e. Global Land Cover Facility-Global Forest Cover Change) product [13,15]	1975, 1990, 2000- 2005	30m – 60m	Forest and non-forest for 1975 and 1990; forest cover and change for 2000 and after.	OA = 91% (SE = 1%) after 1990	Tree cover > 30%
3. GlobeLand30 [12]	2000, 2010	30 m	Ten land cover types	UA = 84%, PA = 92% for forest	Not provided
4. FNF (i.e. Forest/Non-Forest) maps [17]	Annual map (2007 ~ 2010)	25 m	Forest and non-forest	OA = 85% - 95%	Crown cover > 10%, area > 0.5 ha
5. FROM-GLC (i.e. Finer Resolution Observation and Monitoring of Global Land Cover) [14]	2010	30 m	Cropland, forest, grassland, shrubland, wetland, water bodies, tundra, impervious surface, barren land, snow and ice	UA = 80%, PA = 76% for forest	Tree cover > 15% and height > 3m
6. GLC_FCS30 (i.e. Global 30-m Land-Cover with a Fine Classification system) product [16]	2015	30 m	A fine classification system with 30 land cover types	OA = 82.5% for 9 basic land-cover types; OA = 68.7 % for 24 land-cover types	11 forest types with forest cover > 15%

Accuracy measurements include overall accuracy (OA), producer's accuracy (PA), user's accuracy (UA), and standard error (SE).

cover and change (FCC) in Sichuan is needed to analyze the impacts of long-term forest policies [9].

Benefiting from the public opening of the Landsat archive, Landsat datasets have facilitated forest change analysis on a global scale [10]. Many global forest/land cover products have been developed using Landsat imagery or other data at a similar resolution [11]–[17]. Six global products with an overall accuracy (OA) of over 80% and varying in temporal coverage, classification schemes, forest definitions, and accuracies are listed in Table I. However, the accuracy of the global product needs to be estimated for each study area before it is used to derive the regional FC and the corresponding change.

However, land cover changes that occurred before the Landsat era (i.e., the 1970s) are largely unknown [18]. To fill the temporal gap, the declassified spy satellite (DSS), Corona images, acquired during the U.S. Key Hole (KH) missions and released to the public in 1995, provided plenty of observations about the Earth's surface in the 1960s [19]. It had a global coverage and enabled land cover and land use change applications when combined with other satellite data [19]–[21]. However, the application of this legacy data at a large spatial scale has been hindered by difficulties in Corona image processing, and intensive human efforts are required [19]. The challenge remains in the accurate, automated georegistration of Corona images, mainly caused by: 1) large errors in the initial geolocation; 2) variations in the resolution of pixels distributed along and across tracks [22]; 3) drastic land cover changes since the 1960s [19]; and 4) significant geometric distortion introduced by the panoramic design of the camera system and the low orbit of the satellites [23]. To solve the geometric errors in DSS data, existing methods mainly rely on solving the transformation function based on ground control points (GCPs) either manually or automatically collected from reference images [20], [21]. The accuracy depends on the errors in the coordinates of the GCPs, and the efficiency depends on the time consumed in GCP collection [19]. In remote sensing-based land cover change studies, automated, machine learning-based approaches were preferred for georegistration and mapping when applying the Corona images in large area monitoring [24], [25].

The overall goal of this study was to estimate the FC of the Sichuan Province over a forty-year period. A semi-automated image registration method involving an automated tie-point extraction and a matching method for DSS data was proposed. By utilizing Corona data for the 1960s and a Landsat-based FCC product for the 1970s and later, over forty years of FCC for Sichuan Province was derived. The connection between the FCC and the socio-economic factors during the half-century' period were further investigated.

II. STUDY AREA AND DATA

A. Study Area

Sichuan Province, located in southwest China, covering an area of 4.84×10^5 km^2 (see Fig. 1), was defined as the spatial extent of this study. Adjoining the Qinghai-Tibetan Plateau, forests in Sichuan are characterized by high spatial diversity and sensitivity to climate change. Forest carbon density decreases from subalpine coniferous forests in western Sichuan (30–40 MgC·hm^{-2}) to the montane evergreen broadleaf forest located in the east and towards the edge of the Sichuan Basin

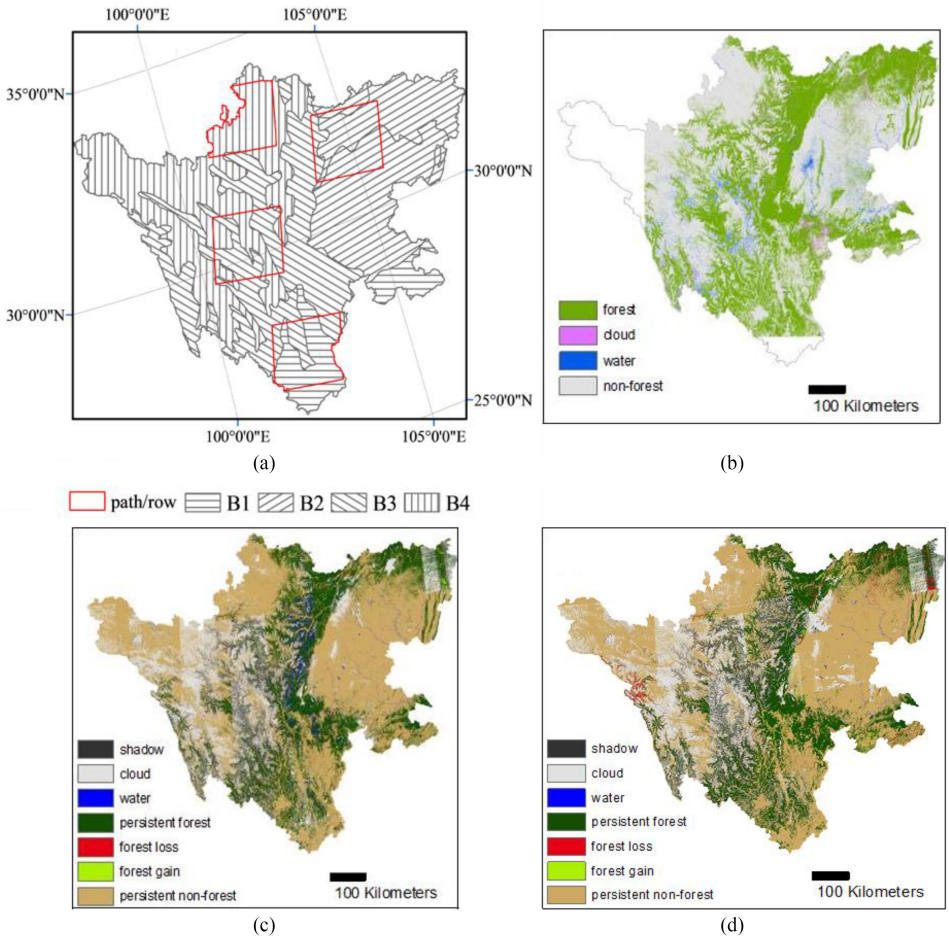

Fig. 1. (a) Location and distributions of biomes in Sichuan. B1: Tropical and subtropical moist broadleaf forests; B2: Temperate broadleaf and mixed forests; B3: Temperate coniferous forests; B4: Montane grasslands and shrublands. The biome data was downloaded from the World Wildlife Fund[1] The path/rows selected for assessing the accuracy of GFCC products were labeled with red frames. (b) GLCF-GFCC maps for Sichuan, including the FC map for 1975. (c) Change maps for 1990–2000, and (d) 2000–2005, provided by the previous Global Land Cover Facility. All maps were projected to the Lambert Azimuthal Equal Area projection.

(20–30 MgC·hm^{-2}), and increases along altitudes and slopes [25]. Chongqing city, which was separated from Sichuan in 1997, was not included in the study area.

B. Satellite Images

1) Corona Images: Corona images were originally recorded on films by panchromatic cameras and then digitized by the USGS to 8-bit radiometric precision [23]. The KH-4A and KH-4B missions, accomplished between the 1960s and the early 1970s, acquired most of the high-quality images, and the satellites launched during these two missions shared similar cameras, platforms, and image parameters. The nominal ground coverage per frame was approximately 17 × 232 km and 13.8 × 188 km for the two satellites respectively [23]. The flying altitudes were around 180 km for the KH-4A satellites and 150 km for the KH-4B satellites, thus, the ground resolution of the images varied across the scan direction, ranging from 2.7 to 7.6 m for KH-4A images and from 1.8 to 7.6 m for KH-4B images. Along the scan direction, the pixels with the finest resolution are located at the center of the images. Forty-six Corona images, acquired during the KH-4A or KH-4B missions, were downloaded to estimate the FC of Sichuan in the 1960s.

2) Landsat Data: Landsat data acquired since the 1970s have a significant temporal continuity with Corona data. The Landsat data collected from the Global Land Survey (GLS) collection were processed with an average error of less 1 Landsat pixel at 30 m resolution among different epochs [18]. Because most GLS 2000 images were acquired by Landsat 7, which was designed to provide better geodetic accuracy than Landsat 5, these images were used as reference data to register the Corona images.

C. FC Products and Statistics

1) Landsat-based FCC Product: Among various FCC products, the Global Forest Cover Change (GFCC) product, made by the previous Global Land Cover Facility (GLCF) [10], [13], [15], [26], [27], was characterized with the longest temporal coverage and the best match of forest definition to statistics; thus, it was selected for analyzing the temporal cover and change trend in Sichuan Province (see Fig. 1). The GLCF-GFCC product mapped forest/non-FC at 60 m resolution for the epoch 1975,

[1][Online]. Available: http://www.worldwildlife.org.

and the changes in forests between 1990, 2000, and 2005 at 30 m resolution. The GLCF-GFCC product was derived from an enhanced GLS data collection during the epochs 1990, 2000, and 2005 [13], [15], [26]. The entire Multi Spectral Scanner (MSS) collection during the 1970s was used to remove gaps of clouds or shadows and to select the best pixel composite; thus, the FC map of nominal 1975 spans a range of years in the 1970s [28].

The GFCC collection also featured consistent forest definition, consistent training, and classification algorithms across different epochs [13], [27]. A tree cover layer at 30 m resolution for the years 2000 and 2005 was generated by integrating the Landsat surface reflectance and the Moderate Resolution Imaging Spectrometer Vegetation Continuous Field data through a regression tree algorithm [27]. Subsequently, FCs in the 2000 and 2005 epochs were derived by translating percent tree data to categorical forest/non-FC using the International Geosphere-Biosphere Program (IGBP) forest definition [29]. As a result, the FC loss and gain between 2000 and 2005 were estimated using a probability-based bi-temporal change detection algorithm (Sexton *et al.* 2015). For the 1990 epoch, stable pixels that were either persistent forest or persistent nonforest between the years 2000 and 2005 were identified and used as training data to classify the FC for 1990 [13]. A similar algorithm was then developed for the 1975 epoch by adding training samples collected from 1990 [28]. The global OA of the forest-cover class and forest-change class were 91% and $> 88\%$, respectively [15]. It should be noted that all maps and satellite data used in this study were projected to the Lambert Azimuthal Equal Area projection.

2) Forest Statistics: Consecutive National Forest Inventories (NFI) were implemented from 1973 to 2008 (1st, 1973–1976; 2nd, 1977–1981; 3rd, 1984–1988; 4th, 1989–1993; 5th, 1994–1998; 6th,1999–2003; and 7th, 2004–2008). The NFI statistics were downloaded from the Chinese Forest Science Data Center (CFSDC),[2] [30]–[32] and the provincial statistical yearbooks.[3] Earlier FC data for 1949 and 1950–62 were obtained from the Thematic Database for Human-Earth System (TDHS),[4] However, it is noteworthy that technical details, especially of the TDHS statistics, were not available.

III. Methodology

The estimation of the multidecadal FCC includes two major sections. The first is the FC estimation for the 1960s using Corona images, and the second is the Landsat-based FC estimation from 1975 to 2005. The workflow is presented in Fig. 2, and each step is elaborated separately in the following sections.

A. FC Estimation for the 1960s

1) Sampling Design: A sampling method is commonly adopted for land cover and change estimation when data availability is limited [33]. Among the different sampling strategies, the stratified random sampling (SRS) method is favored over simple random sampling or systematic sampling because of its advantages in reducing uncertainty and maintaining the accuracy of the estimate [34]. Information on the FCC in the 1960s, especially with explicit spatial distribution, is needed to define the stratum for the SRS method. A FCC probability map was produced using an experiential model. Assuming that FCC after the 1970s, along with other factors such as land cover types, provide a good indication of FCC from the 1960s to the 1970s, a set of independent variables was used to predict the probability of change that happened between the 1960s and the 1970s, denoted as $\mathrm{FCC}_{60s}\%$ in (1). The factors included persistent forest (denoted as $ff\%$) and nonforest ($nn\%$), forest loss ($fn\%$) and gain ($nf\%$) between 2000 and 2005, DEM [35] and fractions of land use types such as crop ($\mathrm{crop}\%$), forest ($f\%$), grass ($\mathrm{grass}\%$), water ($\mathrm{water}\%$), buildup ($\mathrm{buildup}\%$), unused land ($\mathrm{unused}\%$) derived from a land use data produced by the Institute of Geographic Sciences and Natural Resources Research, Chinese Academy of Science. The model was trained in Panzhihua city, located in southern Sichuan, where forest loss happened during the 1960s due to coal mining [36] and was then applied to the entire province. The model was trained at a resolution of 10 km, which was the size of the sample blocks as well as the width of the Corona scene. The prediction model was as follows:

$$\begin{aligned}\mathrm{FCC}_{60s}\% = {} & 1.5 + 0.14 \times ff\% + 3.41 \times fn\% + 1.75 \times nf\% \\ & + 0.17 \times nn\% - 0 \times \mathrm{DEM} - 0.014 \times \mathrm{crop}\% \\ & - 0.014 \times f\% - 0.016 \times \mathrm{grass}\% - 0.011 \times \mathrm{water}\% \\ & - 0.012 \times \mathrm{buildup}\% - 0.136 \times \mathrm{unused}\% \qquad (1)\end{aligned}$$

By applying (1) to the entire study region, the change probability was predicted for all the 10×10 km^2 blocks in Sichuan. Three "change" strata, including low, medium, and high change, represent different degrees of FCC, and a no-change stratum that is located in regions without FC or regions with no valid data due

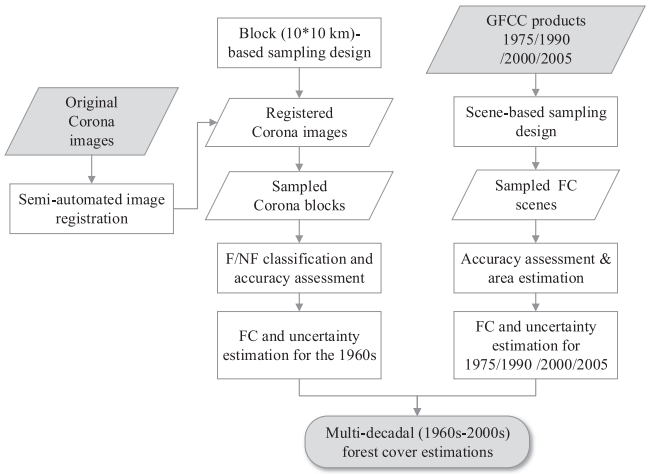

Fig. 2. Flowchart of the multidecadal FCC estimations using satellite data. (F: forest, NF: nonforest, FC: forest cover).

[2][Online]. Available: http://www.cfsdc.org/
[3][Online]. Available:http://www.sc.stats.gov.cn/
[4][Online]. Available: http://www.data.ac.cn/index.asp

TABLE II
SUMMARY OF STRATIFIED SAMPLING DESIGN, INCLUDING THE BOUNDARY, SIZE OF TOTAL POPULATION, SIZE OF SAMPLED BLOCKS, AND THE RATIO OF SAMPLING FOR EACH STRATUM

Stratum (threshold of FCC%)	Percent of area	No. of blocks (N_h)	No. of sampled blocks (n_h)	Percent sampled	Percent of total sampled bocks
No change (<0.078%)	22.64%	1096	10	0.91%	16.67%
Low change (0.078-24%)	23.60%	1143	13	1.14%	21.67%
Medium change (24.01-40%)	41.84%	2026	17	0.844%	28.33%
High change (40.01-99.08%)	11.92%	577	20	3.47%	33.33%
Total	100%	4842	60	1.24%	100%

FCC: forest cover change.

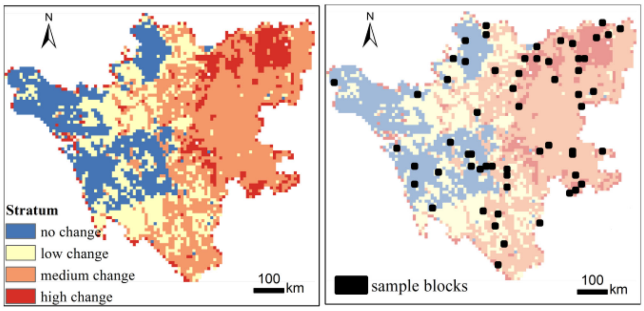

Fig. 3. (a) Strata map and (b) location of selected sample blocks.

to persistent cloud and shadow contamination. The boundaries of strata were derived following the Dalenius-Hodges rule [37], which minimized the coefficients of variation and are listed in Table II.

Furthermore, an optimal allocation method, called the Neyman allocation method [37], was adopted to determine the number of sample blocks to be assigned to each "change" stratum. The distribution of strata and sample blocks are shown in Fig. 3. Ten blocks were selected from the "no-change" stratum. For the three "change" strata, 50 blocks in total were sampled, considering factors such as processing time and image availability. In total, 60 blocks were sampled for the change and no-change strata in Sichuan, representing a sampling ratio of 1.24%. At the same time, 60 Corona images were selected to cover all sample blocks based on the nominal coverage of the Corona image.

2) Semi-Automated Georegistration of Corona Data: The Corona data provided by the USGS were pictures with no geoinformation. In this study, a semi-automated registration procedure for Corona data was developed which includes the following steps.

1) Preliminary registration.
2) Tie points selection.
3) Image transformation.

A full scene was produced first by mosaicking the four subsets using an automated feature-based panoramic image-stitching algorithm [38]. Further, a Corona scene was rotated to a Universal Transverse Mercator projection at a resolution of 30 m. Thus, an initial geolocation was assigned to each Corona scene with a maximum error of 150 Landsat pixels (~4500 m), which enabled a precise image matching procedure against the referenced Landsat data.

Considering the difficulties in collecting ground points for the Sichuan Province, the Scale Invariant Feature Transform (SIFT) [39], [40] algorithm was adopted to automatically search for tie points between the Corona and Landsat images. The SIFT descriptor has been demonstrated to be a robust local invariant feature descriptor for images with different geometrical properties [41], which allows the feature to be matched between multiple images acquired by different satellites or at different time periods. The collected SIFT matches can sometimes contain pseudo matches or do not follow an even distribution. Two key steps were performed to mitigate these impacts. First, the pair of SIFT matches with a geolocation difference of more than 150 pixels at 30 m were considered pseudo matches and were thus excluded. Next, a 2nd-order polynomial transformation function was estimated between the image coordinates of the SIFT points in the Corona and Landsat images. A fitting residual was calculated for each SIFT match. The matched SIFT tie points were considered as "pseudo" matches if their residuals calculated from polynomial functions exceeded a certain threshold. Based on experiments over multiple scenes, the threshold was set to six pixels at 30 m resolution. The search was iterated until a defined threshold was achieved. The coordinates of the refined SIFT features on the Corona and Landsat images were recorded and used to solve the transformation models. A 2nd order polynomial function, which was demonstrated to be feasible when applied to a subset of Corona data [19], was used in this study. The error along two dimensions of an image (i.e., RMSE_X and RMSE_Y) and the total error (i.e., RMSE_{XY}) were calculated to quantify the georegistration accuracy using the following equations:

$$\mathrm{RMSE}_X = \sqrt{\frac{\sum_{i=1}^{n}\left(X_i^C - X_i^L\right)}{n}} \tag{2}$$

$$\mathrm{RMSE}_Y = \sqrt{\frac{\sum_{i=1}^{n}\left(Y_i^C - Y_i^L\right)}{n}} \tag{3}$$

$$\mathrm{RMSE}_{XY} = \sqrt{RMSE_X^2 + RMSE_Y^2} \tag{4}$$

where (X_i^C, Y_i^C) and (X_i^L, Y_i^L) represent the geographic coordinates of the ith ($i = 1, \ldots, n$) selected feature center or tie point from the Corona and Landsat images, respectively.

3) Derivation of Provincial Level FC: A combination of textural features, including dissimilarity, second moment, co-occurrence variance, and mean, is suitable for forest/nonforest classification [19], [42]. In addition, a window size of 7×7 pixels was used for classification in complex landscapes such as Sichuan. Thus, the four textures were calculated at the original resolution of the Corona image and aggregated using a scaling

factor of 7 × 7 pixels. Image classification was implemented using an SVM classifier and then aggregated to 30 m. An OA of over 90% was achieved for the forest/non-forest classification over different blocks; thereby, the fractional rate of FC was derived for each 10 × 10 km^2 sample block and used directly to derive the regional FC. By adopting the methods for calculating the regional estimate from samples [43], the percentage of FC and its standard error over the entire Sichuan Province can be inferred from a sample-based estimation of FC percentage. For each stratum h, a simple random sample of n_h blocks was selected from all blocks, N_h. N is the total number of blocks in Sichuan. The regional average FC rate, $\widehat{\bar{Y}}$, was calculated using the following equation:

$$\hat{\bar{Y}} = \sum_{h=1}^{H} \frac{N_h \bar{y}_h}{N} \tag{5}$$

$$\bar{y}_h = \sum\nolimits_{u \in h} y_u / n_h \tag{6}$$

where $\bar{y}_h$ is the average FC of all selected sample blocks in stratum h, y_u is the FC for each sample block $u(u \in h)$ derived from selected Corona classification maps, H is the number of strata, and *N* is the total number of blocks in Sichuan. The variance $\hat{V}$ of the estimated FC was calculated using the following equation:

$$\hat{V}\left(\hat{\bar{Y}}\right) = \left(\frac{1}{N^2}\right) \sum_{h=1}^{H} \frac{N_h^2 \left(1 - \frac{n_h}{N_h}\right) s_{yh}^2}{n_h} \tag{7}$$

$$s_{yh}^2 = \sum_{u \in h} (y_u - \bar{y}_h)^2 \Big/ (n_h - 1) \tag{8}$$

where S_{yh}^2 is the sample variance of the stratum h. The standard error SE of the estimated regional FC $\widehat{\bar{Y}}$ is the square root of the estimated variance $\hat{V}$.

B. FC Estimation From Landsat Products

1) Accuracy Assessment of FC Products: Accuracies of the GFCC product have conducted at a global scale for epochs after 1990 [15], however, the global accuracies cannot represent the accuracies at a regional scale. Gaps caused by cloud or shadow can be observed from the maps (see Fig. 1), which could affect the calculation of FC. To utilize this dataset, an accuracy assessment needed to be conducted, particularly for Sichuan. Four WRS2 path/rows were randomly selected from a total of 24 paths/rows, representing the four biomes of the region. An SRS algorithm with proportional allocation was adopted with forest and nonforest classes as two strata [44]. A sampling percentage of 0.003% was defined, considering the time and effort required for reference class labeling. Thus, 384 forest pixels and 572 nonforest pixels were randomly sampled from the four forest/nonforest maps of 1975.

Owing to the lack of reference data for the early 1970s, it is unavoidable to use ancillary information to make the best estimation of the forest/nonforest class for the 1970s. Each sample pixel was examined by visually interpreting MSS imagery of the 1970s and high-resolution imagery from Google Earth afterward. Knowledge of the temporal change derived from other GFCC epochs, along with the spatial context of the pixel, was used to label each sample pixel. An assumption for labeling was that from the 1970s to the 1990s, forests were more likely to be disturbed than regrow. Therefore, a pixel is likely to be forest in the 1970s, if it exhibits vegetation characteristics in the MSS image of the 1970s, and is classified as forest in the 1990s and afterward. On the contrary, if a pixel is classified as non-forest after 1990, it may be a forest pixel depending on its spectral characteristics in the MSS image because forest loss could have occurred during the 1970s and the 1990s. The set of reference pixels for 1975 was reserved for assessing the accuracy of the FC maps after 1990.

TABLE III
ERROR MATRIX OF SAMPLE COUNTS (n_{ij}) AND ESTIMATED AREA PROPORTION ($\hat{p}_{ij}$)

Class	Forest	Non-forest	Total
Forest	$n_{11}(\hat{p}_{11})$	$n_{12}(\hat{p}_{12})$	$n_{1\bullet}(\hat{p}_{1\bullet})$
Non-forest	$n_{21}(\hat{p}_{21})$	$n_{22}(\hat{p}_{22})$	$n_{2\bullet}(\hat{p}_{2\bullet})$
Total	$n_{\bullet 1}(\hat{p}_{\bullet 1})$	$n_{\bullet 2}(\hat{p}_{\bullet 2})$	$n(1)$

Map classes are shown in rows while reference classes are in columns.

2) Forest Area Estimation: The common form of the error matrix in terms of sample counts is listed in Table III, accompanied by an unbiased estimator of the proportion of area in cell *i*, *j* of the error matrix:

$$\hat{p}_{ij} = W_i \frac{n_{ij}}{n_{i\bullet}} \tag{9}$$

where W_i is the proportion of area mapped as class *i*. n_{ij} is the count of sample pixels labeled as class *i* in the classification map and as class *j* in the reference map, and $n_{\mathrm{i}\bullet}$ is the count of total samples pixels in class *i* (see Table III). Estimates of accuracy, including user's accuracy (U or UA), producer's accuracy (P or PA), and OA (O or OA), based on the SRS design can be obtained by applying the following equations:

$$\hat{U}_i = \frac{\hat{p}_{ii}}{\hat{p}_{i\bullet}} \tag{10}$$

$$\hat{P}_j = \frac{\hat{p}_{jj}}{\hat{p}_{\bullet j}} \tag{11}$$

$$\hat{O} = \sum_{j=1}^{q} \hat{p}_{jj}. \tag{12}$$

The unbiased estimates of FC and standard error were calculated using the following equations [45]:

$$\hat{p}_{\bullet 1} = \sum_{i=1}^{2} W_i \frac{n_{i1}}{n_{i\bullet}} \tag{13}$$

$$S\left(\hat{p}_{\bullet 1}\right) = \sqrt{\sum_{i=1}^{2} W_i^2 \frac{\frac{n_{ij}}{n_{i\bullet}}\left(1 - \frac{n_{ij}}{n_{i\bullet}}\right)}{n_{i\bullet} - 1}}. \tag{14}$$

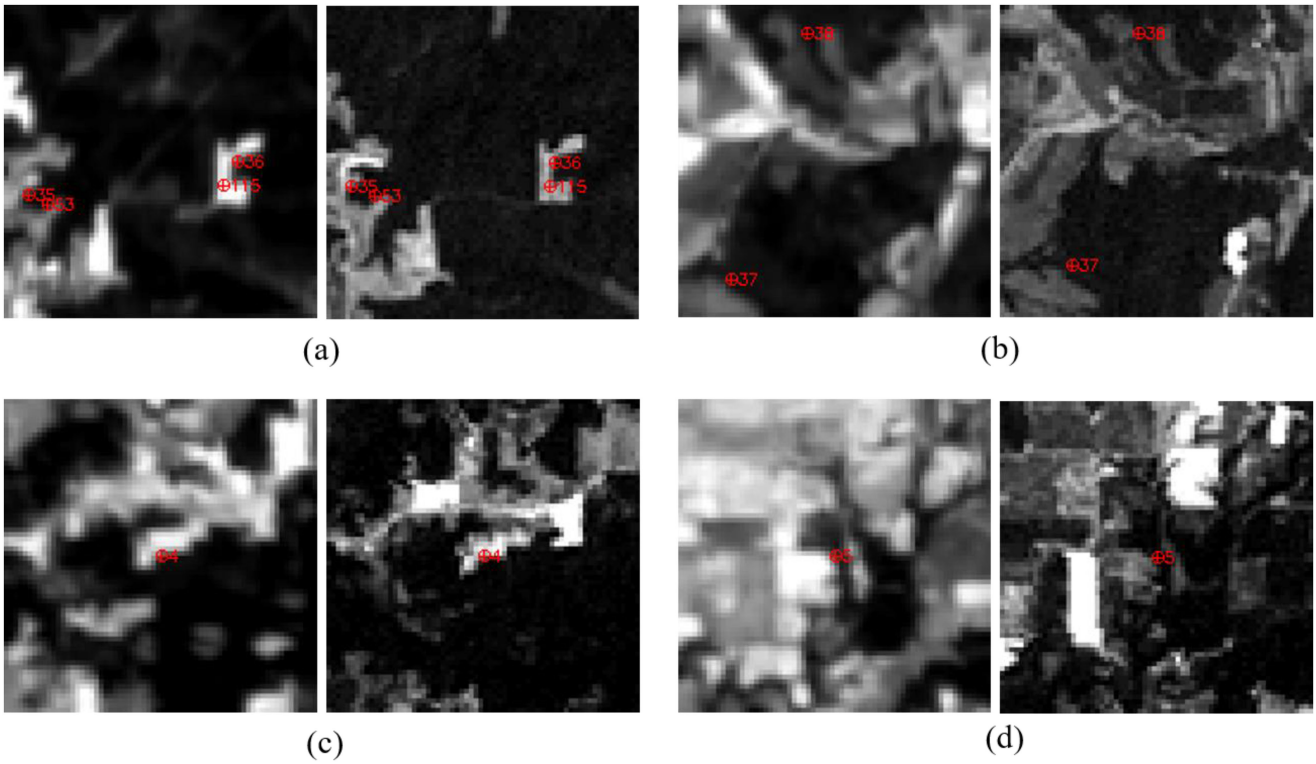

Fig. 4. Red circle-crosses show the refined matching point-pairs selected by SIFT algorithm, the left image is DSS image and the referenced Landsat images (the red band) are presented in the right.

IV. Results

A. Georegistration Accuracy of the Corona Data

After preprocessing, the geolocation difference between the preliminarily registered Corona and reference Landsat images was constrained to less than 4500 m (i.e., ∼150 Landsat 30 m pixels). The SIFT algorithm found features from each individual image and successfully matched pairs of feature points with the largest similarity. The examples in Fig. 4 demonstrate the distribution of refined SIFT matches in a zoomed-in view. In contrast to the feature points usually selected by experts through visual interpretation, SIFT did not tend to select features such as river turning points, mountain ridges, or valleys; instead, the algorithm selected features at multiple scales and finalized the location at the center of a multiscale feature. Although the SIFT features are not as "obvious" as manually selected features, the accuracy is usually high because SIFT reports the location of the feature at the subpixel scale, and the number of feature points is ensured to satisfy the requirements. For instance, the SIFT algorithm exported 677, 625, and 2000 "qualified" matching points for the three subsets of a Corona scene (Corona ID: DS1105-2248DF067). The refinement step reduced the matching points to 183, 279, and 928 (see Fig. 4), respectively, which are still adequate to solve the transformation function. Similar amounts of tie points were generated for other Corona scenes covering the study area. The overall errors after registration were approximately 60–90 m (see Table IV), which were approximately 1–1.5 MSS pixels (60 m), but were much more improved than the preliminary registration.

TABLE IV
Accuracy of Polynomial and Collinear Function Separately Based on Refined SIFT Matching Points

SIFT point set		2nd order polynomial		
Validation experiment	Number of points	RMSE_X (m)	RMSE_Y (m)	RMSE_XY (m)
1	183	34.2	53.7	63.7
2	279	45.6	63.9	78.5
3	928	49.5	75.3	90.1

B. Accuracies of Remote Sensing-Based Forest Cover Classifications

The accuracies of forest/nonforest classification for the 1960s were over 90% across all sample blocks. The accuracy of forest class in 1975 was consistently high across all biomes in Sichuan, with an OA of being 91.5% (SE = 1.57%) (see Table V). The producer's accuracy was >90% and the UA was 88% for the forest class. Therefore, commission errors (CE = 1-UA) and omission errors (OE = 1-PA) were ∼10%. The highest accuracies were found in coniferous forests (p131r039), and temperate forests (p129r038), followed by subtropical moist forests (p130r041) and mountain steppes (p131r037), which respectively had producer's accuracy (PA) of 92.27%, 91.56%, 89.97%, and 80.68%, and UA of 89.72%, 92.14%, 85.34%, and 66.67% for the forest class. The omission errors were < 20%. The accuracies for the 1990 epoch and later were consistent with the map of 1975, with an OA of ∼94% for all maps. The UA for the forest class was consistently over 90%, and the producer's

TABLE V
ACCURACY OF FOREST CLASS FOR GLCF-GFCC PRODUCT AT FOUR EPOCHS IN SICHUAN. THE BIOME WHERE EACH LANDSAT SCENE LOCATED IS ALSO SHOWN

Validation Sites and Accuracy Measures		1975	1990	2000	2005
p131r039 Coniferous forest	*UA*	89.72	96.67	100.00	93.33
	PA	92.27	91.44	95.92	91.57
	OA	92.84	97.15	99.04	96.59
p129r038 Temperate forest	*UA*	92.14	91.40	95.95	93.24
	PA	91.56	94.87	79.96	82.88
	OA	91.64	94.32	89.20	90.13
p130r041 Subtropical forest	*UA*	85.34	92.54	98.55	98.55
	PA	89.97	83.64	83.33	87.12
	OA	87.22	89.49	91.05	93.28
p131r037 Mountain steppe	*UA*	66.67	88.24	94.44	94.12
	PA	80.68	60.02	72.47	55.28
	OA	95.24	97.65	98.54	97.29
Total	*UA*	88.02	92.27	97.40	95.26
	PA	90.91	88.63	83.13	84.64
	OA	**91.52**	**94.34**	**93.69**	**93.86**

Accuracy measurements include OA, producer's accuracy (PA), and UA of the Forest Class.

TABLE VI
PERCENT FOREST COVER (%) FROM 1960S TO 2005 ESTIMATED FROM REMOTE SENSING DATA AND STATISTICS OF FOREST INVENTORY

Epochs	**RS-based FC** (se)	**NFI stats**			**Yearbook**		**TDHS**	
		FC	Forest land use	Forested land	FC	Forested land	Forest land use	Forested land
1949	-	-	-	-	-	-	-	16.92
1960s	**45.19** (1.62)	-	-	-	-	-	36.31	12.89
Circa 1975 (1st NFI)	**38.98** (2.06)	13.3	36.04	13.26	-	-	-	-
Circa 1990 (4th NFI)	**28.91** (2.07)	20.37	47.21	20.37	19.17	-	-	-
Circa 2000 (6th NFI)	**28.19** (2.27)	30.27	46.84	25.51	39.7	24.23	-	-
Circa 2005 (7th NFI)	**27.87** (2.14)	34.31	47.79	27.15	28.98	27.13	-	-

Standard error (i.e., SE) associated with forest cover is reported in parentheses (FC: Forest Cover).

accuracy was slightly lower, ranging from 83.13% in 2000 to 88.63% in 1990.

C. Forest Cover Change Estimates

The results in Table VI reflect the estimates of the forest cover rate for Sichuan from the 1960s to 2005. For comparison, the percentages of forest cover, forestland, and forest land use reported from three sources, including NFI, Yearbook of Sichuan Province, and TDHS, are provided. An estimated forest cover of 45.19 $\pm$ 3.11% in the 1960s was derived from the sampled Corona classification maps at 95% confidence level. Using the GFCC product of circa 1975 yielded an estimated forest cover of 38.98 $\pm$ 4.04% at 95% confidence level. For the following epochs, GFCC products also yielded area-adjusted estimates of forest cover of 28.20 $\pm$ 4.06%, 27.73 $\pm$ 4.45%, and 27.27 $\pm$ 4.19% at 95% confidence level in 1990, 2000, and 2005, respectively. Fig. 5 further illustrates three examples of changes in Sichuan's forest cover over a 40-year period observed from Corona, MSS, TM, and ETM+ images, including 1) deforestation due to mining (circa 2000), 2) deforestation (circa 1990) and regrowth (since 2000), and 3) conversion of forest to cropland (since 1990). The continuous decrease in forest cover during the 40-year period monitored by remote sensing data showed that forest cover has totally decreased by 38% from the 1960s to 2005 in Sichuan. Thirty-one percent of the total forest loss was during the first decade (circa 1965–1975), and 58% occurred between 1975 and 1990. Since 1990, forest cover had become relatively stable, with a much lower decrease rate of 0.24% per year until 2005.

The forest cover estimates reported by NFI, the Statistical Yearbook Series of Sichuan Province, and TDHS are quite different from the remote sensing-based estimates. Other measurements reported in each dataset to measure the area of forest, such as forest land use and forest land, and the differences in definitions are further presented in the discussion section. Only TDHS statistics contained forest cover before the 1960s, reporting rough estimates of 16.92% of forestland in 1949 and 36.31% of forest land use in the early 1960s. The percentage of forest cover reported by NFI stats was 13.3% in the 1970s, which increased to 20.37% until circa 1990. The 6th NFI conducted around 2000 shows a forest cover of 30.27%, which increased to 34.31% in circa-2005 according to the 7th NFI statistics.

TABLE VII
LIST OF KEY FOREST AND RELEVANT POLICIES IN CHINA FROM LATE 1950S TO 2000S

Key socioeconomic periods	**Key Forest Policies**
1958-1962 Rapid Development Period	Establishment of People's Commune (1958) The Second Five Year Plan (1958-1962)
1963-1977 Pre-Economic Reform Period	"Who plants, who owns" Regulation (1964) National Forestry Development Plan (1971)
1978-1998 Economic Reform Period	Green Great Wall program (1978) Household Production Responsibility System (1977 – 1991) The Forest Ownership Policy (1981) Forestry Law (1985) Forestry Reform (1992-1998)
1998-2010 National Afforestation and Deepened Reform Period	Natural Forest Conservation Program (1998-2050) Grain to Green Program (GTGP) (since 1999) Deepened Forestry Reform (since 2003)

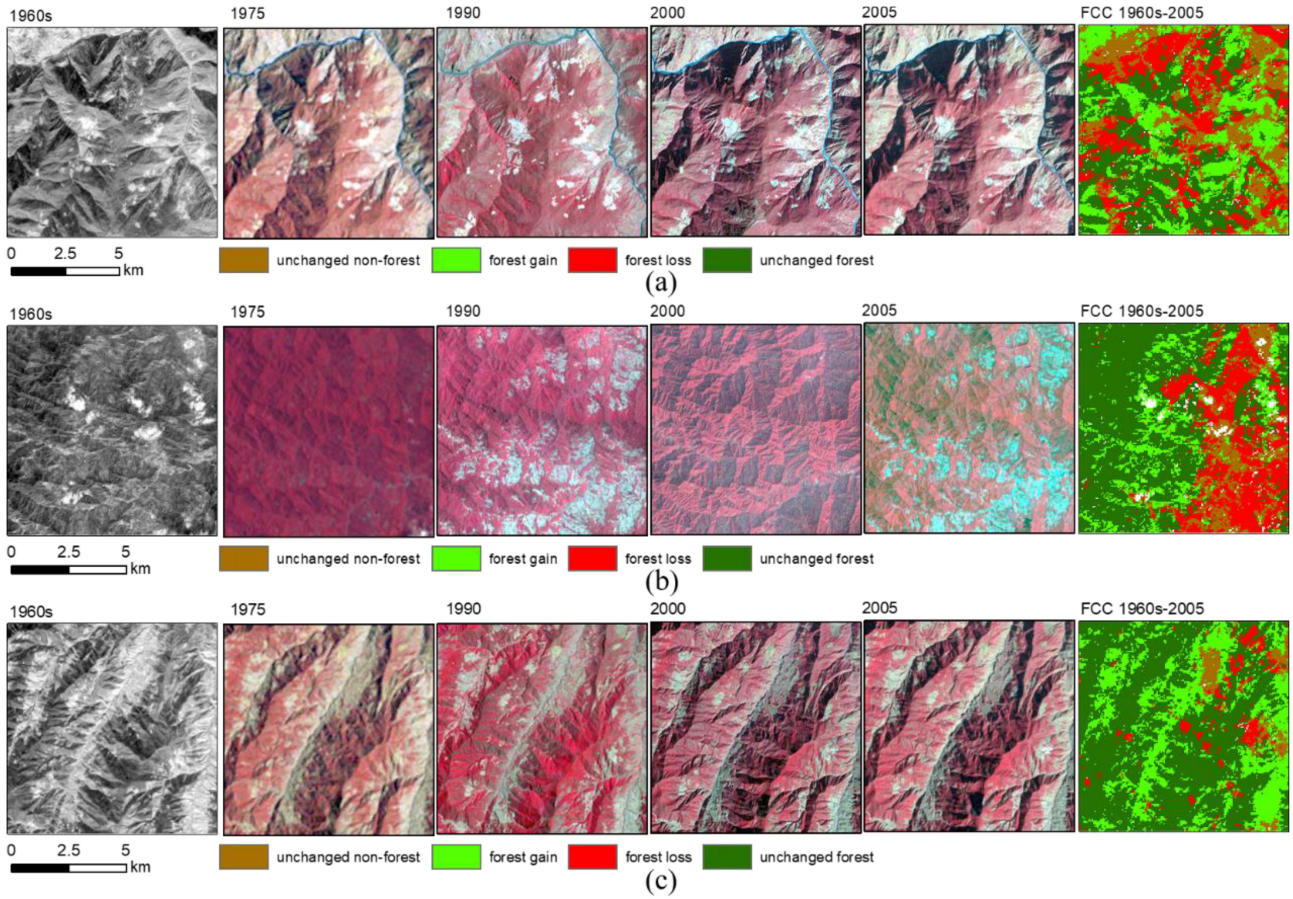

Fig. 5. Three examples demonstrate different types of FCC processes in Sichuan. Each group of images includes a declassified Corona data, a false-color composited Landsat image for each epoch respectively and a map showing the forest cover change occurred during the period between the 1960s and 2005.

During the next decade, the forest cover in Sichuan continuously increased from 35.22% in circa-2010 [46] to 38.03% reported in the latest 9th NFI statistics in 2018.[5]

Overall, forest cover increased by 158% from the 1970s to 2005, with 66% of the total increase occurring after 1990. The Sichuan Statistical Yearbook reports an increasing trend from 19.17% of forest cover in 1990 to 39.7% in 2000 and a decreasing trend to 28.98% in 2005. It should be noted that Chongqing City was separated from Sichuan province in 1997; thus, the statistics of forest cover reported for years earlier than 1997 included the forests in Chongqing.

V. Discussion

Large-scale forest cover changes occurred worldwide as a result of WWII [20], and long records of changes are needed to understand the contributions of historical land use change to carbon fluxes and the loss of biodiversity. DSS data allow the extension of Landsat-based estimates back to the 1960s for most areas of the globe. A major challenge in applying the Corona data in global land cover estimations is georegistration, especially the collection of GCPs. The developed registration method can significantly improve the efficiency of achieving effective geolocation accuracy by automatically collecting feature points, which is a key step in using DSS data to map forest cover over very large areas. However, there are still unsolved issues hindering the full automation of the DSS images registration and thus the pixel-level mapping against other satellite products. The major challenges are in collecting and matching feature points due to the land cover changes.

Forest cover change in Sichuan, revealed by DSS-Landsat, are likely driven by socio-economic events and policies Table VII. Forest policies have various impacts on changes of forest area and management intensity, as a result of creating secure or insecure tenure systems, changing incentives for forest production, affecting timer price and taxes, and reforestation/afforestation programs [47], [48]. As a pioneer region for several forestry programs [3], Sichuan, with its forest cover change could reflect the effects of forest policies over different time periods. From the 1960s to the mid-1970s, forest cover decreased by 13.7%, which could be explained by the tenure system of forest land and timber output from forests. From a tenure perspective, forest degradation was mainly due to the lack of confidence in tenure security caused by frequent changes in forest policies in the 1960s [49]. Exploiting of forest resources was recorded and rampant timber cutting occurred around the nation, at the same time; furthermore, afforestation campaigns were highly inefficient, with nominal surviving rate of only 20% [7]. From a

[5][Online]. Available:www.forestry.gov.cn

financial perspective, the forest sector in China mainly supplied underpriced timber products to support national economic development during the three decades before 1978 [7]. Deforestation in Sichuan as a whole began in the 1950s, and in its major forested regions such as Aba Prefecture in the 1960s, when it supplied about 84% of the timber output of the province, and Garzê Tibetan Autonomous Prefecture [36], [50].

Continuous deforestation from the mid-1970s to the late 1990s was monitored by satellite observations. Since 1978, economic reforms have been carried out in the country. In 1985, the Forestry Law was finalized, which opened the timber market to meet the demand for timber products during the period of rapid economic development. State-owned forest companies became more autonomous with increasing controls on timber production. Meanwhile, collectively owned woodlands were distributed to peasants, with entitlements to harvest forest land [7]. In Sichuan, the forest destruction is the most severe along river or highways due to multiple factors, such as transportations, damn constructions or geo-hazards [51]. Forest cover has been estimated to decrease from 30% in the 1950s to 14% in the 1980s [52] in western Sichuan, which hosts most of the conifer forests.

The drastic demise of forest cover ceased in the late 1990s, and the forest cover in Sichuan stabilized at around 27% after 2000, which could be attributed to the national afforestation programs and conservation activities such as logging bans in important forest regions such as Sichuan. The NFCP, which was carried out in Sichuan since 1998, was characterized by a strict logging ban in natural forests and incentive afforestation. The duty of most employed in the forest sector has shifted from logging to tree planting [3]. Afforestation accounted for 2.34 million ha in Sichuan from 1989 to 2000. NFI statistics reported a continuous growth in the forest cover in Sichuan, which increased from 35.22% to 38.03% during the decade since 2008 [46].[6] However, remote sensing data could not yet provide observational evidence for the continuous net increase in forest cover, as reported by the NFI [53]. It may take more than five years for the large-scale afforestation of the late 1990s to be observable by remote sensing data. Some recent remote sensing-based multitemporal land cover products, for example, Chen *et al.* [12] and Zhang *et al.* [16], could be used to verify the forest gain.

Although remote sensing has provided continuous observations throughout the past several decades, large differences between remote sensing-based forest cover change estimates and statistical reports highlight the challenges in reconstructing historical land use changes for carbon and other studies. On one hand, some of the differences may be due to the use of different definitions and spatial boundaries when measuring the amount of forest. As shown in Fig. 6, the forest cover included shrubland in addition to the forested land, and forest land use included the land with no-standing trees. The separation of Chongqing City could have also caused uncertainties when comparing forest percentages among different epochs. Instead of policy factors, natural factors, such as climate patterns, wildfires, landslides, earthquakes, and

[6][Online]. Available: www.forestry.gov.cn

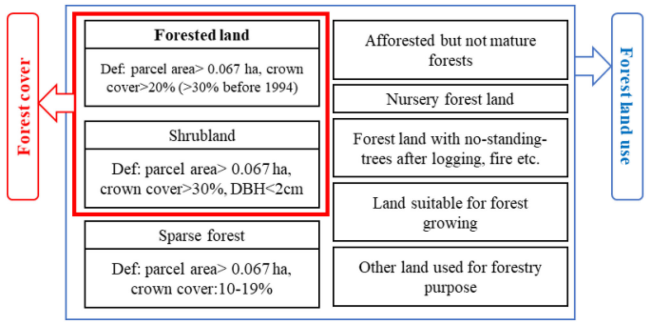

Fig. 6. Definitions of multiple forest measurements, including "forested land", "forest cover" and "forest land use."

so on would also have influences on the forest inventory. On the other hand, large differences among the NFI and yearbook suggest that at least one, but more likely, both, have substantial reporting errors. Such reporting errors are not limited to Sichuan Province or China; estimates on the forest cover change from the Food and Agriculture Organization of the United Nations are deemed erroneous for many countries and regions [54]. Although the DSS-Landsat results are also subject to mapping errors, most of the biases arising from these errors can be corrected through design-based accuracy assessment [45], [55], [56]. Therefore, carefully developed, satellite-based forest cover change products with statistically valid accuracy estimates, if available, should be preferred over government statistical reports in reconstructing historical land use history [57], [58]. Differences between satellite-based results and government reports likely represent the minimum uncertainties in reports available for the years before the satellite results became available.

VI. Conclusion

In this study, the multidecadal forest cover change was monitored using long-term remote sensing observations, including DSS data in the 1960s and Landsat products since the 1970s for Sichuan Province. Note that Sichuan Province has twice the area of the United Kingdom and a population of 84 million compared with the U.K.'s 68 million. The automation of georegistration of historical Corona data was carried out using a novel approach that utilized the SIFT for tie point extraction with Landsat images as references. SIFT feature selection method successfully selected adequate matching points to solve the transformation function. The proposed method enables a sample-based estimation of forest cover over a large spatial area for the 1960s, extending the forest cover mapping from the Landsat era to the 1960s with prospects to achieve full automation of the Corona image registration. The proposed methodologies can be utilized in other provinces or regions for the long-term forest cover change analysis.

Combined with the Landsat-based forest cover change products, a rapid forest loss with a total amount of 38% was estimated for Sichuan during the 40+ years period from the 1960s to 2005. The different changing stages before and after the 1990s revealed the actual impacts of concurrent forestry policies and

socioeconomic factors on forest resources at different time periods. The policies in the 1970s and 1980s, such as the National Forestry Development Plan and Forest Ownership Policy, aimed at serving timber products and caused great losses to the forests. Thereafter, a series of conservation policies were legislated against logging since the late 1990s, which played positive roles in ceasing the forest losses.

Note that, unlike traditional official estimates, the remote sensing-based methods were identical for all dates, with consistent forest definitions and mapping algorithms, as well as a precise depiction of the spatial distribution of changes along with uncertainty estimates. More forest changes were captured by the satellite observations than the official statistics, mainly because the statistics were not primarily based on sampling but comprehensive coverage provided by remote sensing data.

ACKNOWLEDGMENT

The authors gratefully acknowledge data support from the National Earth System Science Data Center, National Science & Technology Infrastructure of China.[7]

REFERENCES

[1] H. J. Albers, S. D. Rozelle, and L. Guo, "China's forests under economic reform: Timber supplies, environmental protection, and rural resource access," *Contemporary Econ. Policy*, vol. 16, no. 1, pp. 22–33, 1998.

[2] J. Liu, M. Linderman, Z. Ouyang, L. An, J. Yang, and H. Zhang, "Ecological degradation in protected areas: The case of Wolong Nature Reserve for giant pandas," *Science*, vol. 292, no. 5514, pp. 98–101, 2001.

[3] J. Liu, S. Li, Z. Ouyang, C. Tam, and X. Chen, "Ecological and socioeconomic effects of China's policies for ecosystem services," *Proc. Nat. Acad. Sci. United States Amer.*, vol. 105, no. 28, pp. 9477–9482, 2008.

[4] E. J. Lindquist *et al.*, "FAO and JRC, global forest land-use change 1990–2005," Food and Agriculture Organization of the United Nations and European Commission Joint Research Centre Rome, 2012.

[5] J. Fang, A. Chen, C. Peng, S. Zhao, and L. Ci, "Changes in forest biomass carbon storage in China between 1949 and 1998," *Science*, vol. 292, no. 5525, pp. 2320–2322, 2001.

[6] C. Chen *et al.*, "China and India lead in greening of the world through land-use management," *Nature Sustain.*, vol. 2, no. 2, pp. 122–129, 2019.

[7] S. Wang, G. C. van Kooten, and B. Wilson, "Mosaic of reform: Forest policy in post-1978 China," *Forest Policy Econ.*, vol. 6, no. 1, 2004.

[8] C. D. Huang, J. Zhang, W. Q. Yang, X. Tang, and A. J. Zhao, "Dynamics on forest carbon stock in Sichuan Province and Chongqing City," *Acta Ecologica Sinica*, no. 3, pp. 966–975, 2008.

[9] A. Viña, W. J. Mcconnell, H. Yang, Z. Xu, and J. Liu, "Effects of conservation policy on China's forest recovery," *Sci. Adv.*, vol. 2, no. 3, 2016.

[10] J. R. Townshend *et al.*, "Global characterization and monitoring of forest cover using Landsat data: Opportunities and challenges," *Int. J. Digit. Earth*, vol. 5, no. 5, pp. 373–397, 2012.

[11] M. C. Hansen *et al.*, "High-resolution global maps of 21st-century forest cover change," *Science*, vol. 342, no. 6160, pp. 850–853, 2013.

[12] J. Chen *et al.*, "Global land cover mapping at 30 m resolution: A POK-based operational approach," *ISPRS J. Photogramm. Remote Sens.*, vol. 103, pp. 7–27, 2015.

[13] D.-H. Kim *et al.*, "Global, Landsat-based forest-cover change from 1990 to 2000," *Remote Sens. Environ.*, vol. 155, pp. 178–193, 2014.

[14] P. Gong *et al.*, "Finer resolution observation and monitoring of global land cover: First mapping results with Landsat TM and ETM+ data," *Int. J. Remote Sens.*, vol. 34, no. 7, pp. 2607–2654, 2013.

[15] M. Feng *et al.*, "Earth science data records of global forest cover and change: Assessment of accuracy in 1990, 2000, and 2005 epochs," *Remote Sens. Environ.*, vol. 184, pp. 73–85, 2016.

[16] X. Zhang *et al.*, "GLC_FCS30: Global land-cover product with fine classification system at 30m using time-series Landsat imagery," *Earth Syst. Sci. Data*, vol. 13, no. 6, pp. 2753–2776, 2021.

[17] M. Shimada *et al.*, "New global forest/non-forest maps from ALOS PALSAR data (2007-2010)," *Remote Sens. Environ.*, vol. 155, pp. 13–31, 2014.

[18] G. Gutman, C. Huang, G. Chander, P. Noojipady, and J. G. Masek, "Assessment of the NASA–USGS Global Land Survey (GLS) datasets," *Remote Sens. Environ.*, vol. 134, pp. 249–265, 2013.

[19] D. X. Song, C. Huang, J. O. Sexton, S. Channan, M. Feng, and J. R. Townshend, "Use of Landsat and Corona data for mapping forest cover change from the mid-1960s to 2000s: Case studies from the Eastern United States and Central Brazil," *ISPRS J. Photogramm. Remote Sens.*, vol. 103, pp. 81–92, 2015.

[20] M. D. Nita, C. Munteanu, G. Gutman, I. V. Abrudan, and V. C. Radeloff, "Widespread forest cutting in the aftermath of World War II captured by broad-scale historical Corona spy satellite photography," *Remote Sens. Environ.*, vol. 204, pp. 322–332, 2018.

[21] Z. Rendenieks, M. D. Nita, O. Nikodemus, and V. C. Radeloff, "Half a century of forest cover change along the Latvian-Russian border captured by object-based image analysis of Corona and Landsat TM/OLI data," *Remote Sens. Environ.*, vol. 249, 2020, Art. no. 112010.

[22] H. G. Sohn, G. H. Kim, and J. H. Yom, "Mathematical modelling of historical reconnaissance corona KH-4B imagery," *Photogramm. Rec.*, vol. 19, no. 105, pp. 51–65, 2004.

[23] N. Galiatsatos, "The shift from film to digital product : Focus on CORONA imagery," *Photogrammetrie - Fernerkundung - Geoinf.*, vol. 3, pp. 251–260, 2009.

[24] J. Casana, "Global-scale archaeological prospection using CORONA satellite imagery: Automated, crowd-sourced, and expert-led approaches," *J. Field Archaeol.*, vol. 45, pp. S89–S100, 2020.

[25] C. D. Huang *et al.*, "Spatial difference characteristics of forest vegetation carbon stock in Sichuan Province," *Acta Ecologica Sinica*, vol. 29, no. 9, pp. 5115–5121, 2009.

[26] S. Channan *et al.*, "The GLS+: An enhancement of the global land survey datasets," *Photogramm. Eng. Remote Sens.*, vol. 81, no. 7, pp. 521–525, 2015.

[27] J. O. Sexton *et al.*, "Global, 30-m resolution continuous fields of tree cover: Landsat-based rescaling of MODIS vegetation continuous fields with lidar-based estimates of error," *Int. J. Digit. Earth*, vol. 6, no. 5, pp. 427–448, 2013.

[28] M. Feng, J. O. Sexton, S. Channan, and J. R. Townshend, "Forest cover of North America in the 1970s mapped using Landsat MSS data," in *Proc. AGU Fall Meeting Abstr.*, 2015, pp. 427–448.

[29] A. S. Belward, "The IGBP-DIS global 1 km land cover data set 'DISCover': Proposal and implementation plans," in *Report of the Land Cover Working Group of IGBP-DIS*. Toulouse, France: IGBP-DIS Office, 1996.

[30] SFA, state forestry administration of china: the seventh national forest resource inventory report (2004-2008). Beijing, China, 2009.

[31] Thematic Database for Human-Earth System, Forest Inventory Data. [Online]. Available: http://www.data.ac.cn/index.asp

[32] SFA, state forestry administration of china: the sixth national forest resource inventory report (1999-2003). Beijing, China, 2005.

[33] M. C. Hansen *et al.*, "Humid tropical forest clearing from 2000 to 2005 quantified by using multitemporal and multiresolution remotely sensed data," *Proc. Nat. Acad. Sci. United States Amer.*, vol. 105, pp. 9439–9444, 2008.

[34] M. Broich, S. V. Stehman, M. C. Hansen, P. Potapov, and Y. E. Shimabukuro, "A comparison of sampling designs for estimating deforestation from Landsat imagery: A case study of the Brazilian Legal Amazon," *Remote Sens. Environ.*, vol. 113, no. 11, pp. 2448–2454, 2009.

[35] USGS, "Shuttle radar topography mission, 1 arc second scene, SRTM_u03_n008e004, unfilled unfinished 2.0," Global Land Cover Facility, Univ. Maryland, College Park, MD, USA, Feb. 2000.

[36] Chinese Academy of Forestry, "Review of forest resources in Sichuan," 2016. Cited 2016 Aug 24. [Online]. Available: http://www.lknet.ac.cn/qz/scsl.htm

[37] W. G. Cochran, *Sampling Techniques*, 3rd ed. New York, NY, USA: Wiley, 1977.

[38] M. Brown and D. G. Lowe, "Automatic panoramic image stitching using invariant features," *Int. J. Comput. Vis.*, vol. 74, no. 1, pp. 59–73, 2007.

[39] D. G. Lowe "Object recognition from local scale-invariant features," in *Proc. 7th IEEE Int. Conf. Comput. Vis.*, 1999, pp. 1150–1157.

[7] [Online]. Available: http://www.geodata.cn

[40] D. G. Lowe, "Distinctive image features from scale-invariant keypoints," *Int. J. Comput. Vis.*, vol. 60, no. 2, pp. 91–110, 2004.
[41] K. Mikolajczyk and C. Schmid, "Scale & affine ivariant interest point detectors," *Int. J. Comput. Vis.*, vol. 60, no. 1, pp. 63–86, 2004.
[42] R. Spiekermann, M. Brandt, and C. Samimi, "Woody vegetation and land cover changes in the Sahel of Mali (1967-2011)," *Int. J. Appl. Earth Observ. Geoinf.*, vol. 34, pp. 113–121, 2015.
[43] S. V. Stehman, "Estimating area and map accuracy for stratified random sampling when the strata are different from the map classes," *Int. J. Remote Sens.*, vol. 35, no. 13, pp. 4923–4939, 2014.
[44] P. Olofsson *et al.*, "Good practices for estimating area and assessing accuracy of land change," *Remote Sens. Environ.*, vol. 148, pp. 42–57, 2014.
[45] P. Olofsson, G. M. Foody, S. V. Stehman, and C. E. Woodcock, "Making better use of accuracy data in land change studies: Estimating accuracy and area and quantifying uncertainty using stratified estimation," *Remote Sens. Environ.*, vol. 129, pp. 122–131, 2013.
[46] "SFA, State Forestry Administration (SFA): The Eighth National Forest Resource Inventory Report (2009-2013)," 2013.
[47] R. Yin and D. H. Newman, "Impacts of rural reforms: The case of the Chinese forest sector," *Environ. Develop. Econ.*, vol. 2, no. 3, pp. 291–305, 1997.
[48] Y. Q. Zhang, J. Uusivuori, and J. Kuuluvainen, "Econometric analysis of the causes of forest land use changes in Hainan, China," *Can. J. Forest Res.-Revue Canadienne De Recherche Forestiere*, vol. 30, no. 12, pp. 1913–1921, 2000.
[49] D. C. Liu, "Tenure and management of non-state forests in China since 1950—A historical review," *Environ. Hist.*, vol. 6, no. 2, pp. 239–263, 2001.
[50] J. P. Hayes, *A Change in Worlds on the Sino-Tibetan Borderlands: Politics, Economies, and Environments in Northern Sichuan*. Plymouth, England: Lexington Books, 2013.
[51] P. Cui, Y.-M. Lin, and C. Chen, "Destruction of vegetation due to geo-hazards and its environmental impacts in the Wenchuan earthquake areas," *Ecological Eng.*, vol. 44, pp. 61–69, 2012.
[52] G. E. Clarke, "Development, Society and Environment in Tibet," pp. 1–45, 1998.
[53] M. C. Hansen, S. V. Stehman, and P. V. Potapov, "Quantification of global gross forest cover loss," *Proc. Nat. Acad. Sci. United States Amer.*, vol. 107, no. 19, pp. 8650–8655, 2010.
[54] X.-P. Song *et al.*, "Global land change from 1982 to 2016," *Nature*, vol. 560, no. 7720, pp. 639–643, 2018.
[55] S. V. Stehman, "Estimating area from an accuracy assessment error matrix," *Remote Sens. Environ.*, vol. 132, pp. 202–211, 2013.
[56] D. He, Q. Shi, X. Liu, Y. Zhong, and X. Zhang, "Deep subpixel mapping based on semantic information modulated network for urban land use mapping," *IEEE Trans. Geosci. Remote Sens.*, to be published.
[57] L. P. Chini *et al.*, "LUH2-ISIMIP2b harmonized global land use for the years 2015-2100," ORNL Distrib. Act. Arch. Center, Oak Ridge, TN, USA, 2020.
[58] Q. Shi, M. Liu, S. Li, X. Liu, F. Wang, and L. Zhang, "A deeply supervised attention metric-based network and an open aerial image dataset for remote sensing change detection," *IEEE Trans. Geosci. Remote Sens.*, to be published. doi: 10.1109/TGRS.2021.3085870.

Dan-Xia Song received the B.S. degree in geographical information sciences from Hohai University, Nanjing, China, in 2007, and the Ph.D. degree in geography from the Department of Geographical Sciences, University of Maryland, College Park, MD, USA, in 2016.

From 2016 to 2018, she was with the 6th Grain Digital Agriculture Company. Since 2018, she has been an Associate Professor with the College of Urban and Environmental Sciences, Central China Normal University, Wuhan, China. Her research interests include the remote sensing based forest cover change monitoring and estimation of vegetation parameters.

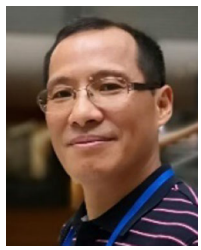

Chengquan Huang received the B.S. in geology, and M.S. in environmental sciences from Peking University, Beijing, China, and the Ph.D. degree in geography from the University of Maryland, College Park, MD, USA.

He is a Research Professor with the Department of Geographical Sciences, University of Maryland, His research interests include remote sensing based land cover mapping, change detection, and the quantification of vegetation biophysics, and related applications in climate, carbon, biodiversity, and resources management.

Tao He received the B.E. degree in photogrammetry and remote sensing from Wuhan University, Wuhan, China, in 2006, and the Ph.D. degree in geography from the University of Maryland, College Park, MD, USA, in 2012.

He is currently a Professor with the School of Remote Sensing and Information Engineering, Wuhan University, Wuhan, China, and also with the Department of Geographical Sciences, University of Maryland. His research interests include surface anisotropy and albedo modeling, surface radiation budget, data fusion of satellite products, and long-term regional and global surface radiation budget analysis.

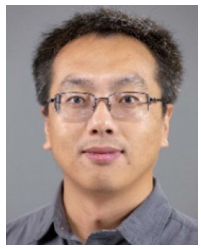

Min Feng received the B.S. degree in physical geography, the M.S. and Ph.D. degrees in cartography and geographic information system from Lanzhou University, Lanzhou, China, in 2002, 2005 and 2008, respectively.

He is a Professor with the Institute of Tibetan Plateau Research, Chinese Academy of Sciences (CAS), Beijing, China. He worked at the University of Maryland and the Institute of Geographic Sciences and Natural Resources Research, CAS after completing the Ph.D. degree. He was also a Senior Researcher with the Global Land Cover Facility (GLCF) and a Visiting Scholar with the UNEP Sioux Falls Center. He was appointed as a Geospatial Consultant to the World Bank. His research interests include remote sensing big data, land cover applications of remote sensing in global forest, and water mapping.

Ainong Li (Member, IEEE) received the M.S. degree in cartography and geographic information system and the Ph.D. degree in physical geography from the Institute of Mountain Hazards and Environment (IMHE), Chengdu, China, in 2004 and 2007, respectively.

From 2008 to 2010, he was a Visiting Research Scientist with the Department of Geography, University of Maryland, College Park, MD, USA. Since 2010, he has been a Professor with IMHE. His research interests include mountain quantitative remote sensing and ecological modeling.

Sike Li received the B.S. degree (with honors) in GIS, in 2015, and the M.S. degree in geographical sciences from University of Maryland, College Park, MD, USA, in 2016. She is currently working toward the Ph.D. degree in geography with the School of Earth Atmosphere, and Environment, Monash University, Melbourne, VIC, Australia.

Her current research interests include using remote sensing application, GIS techniques, and decision.]support system modeling for improving grassland curing degree calculations, with focus on vegetation monitoring and land cover land use change detection analysis.

Yong Pang received the B.S. degree in forestry from Anhui Agriculture University, Hefei, China, in 1997, the M.Agr. degree in forest management from the Chinese Academy of Forestry, Beijing, China, in 2000, and the Ph.D. degree in cartography and geography information system from the Chinese Academy of Sciences, Beijing, China, in 2006.

From 2006 to 2008, he was a Postdoctoral Researcher with the Department of Forest, Rangeland, and Watershed Stewardship, Colorado State University, Fort Collins, CO, USA. He is currently a Professor with the Research Institute of Forest Resource Information Techniques, Chinese Academy of Forestry. His research interests include surface height and vegetation spatial structure from InSAR and light detection and ranging (LiDAR), modeling of LiDAR waveforms from forest stands, and development of algorithms for forest parameter retrieval from remote sensing data.

Hao Wu received the B.S. in survey engineering and M.S. in geodesy and survey engineering degrees from the School of Geodesy and Geomatics, Wuhan University, Wuhan, China, in 2000 and 2003, respectively, and the Ph.D. degree in cartography and GIS from the State Key Laboratory of Information Engineering in surveying, mapping, and remote sensing, Wuhan University, in 2007.

He is currently a Professor with the College of Urban and Environmental Sciences, Central China Normal University, Wuhan, China. His research interests include land use change and earth observation science and its applications.

Abdul Rashid Mohamed Shariff received his B.S. in Surveying from the University Technology Malaysia, Johor, Malaysia, in 1983, M.Sc. degree in cadastre and land information management from the University of East London, London, U.K., in 1990, and the Ph.D. degree in spatial information science and engineering from the University of Maine, Orono, ME, USA, in 1996.

He is with the Department of Biological and Agricultural Engineering, Faculty of Engineering, Universiti Putra Malaysia, Selangor, Malaysia. His research focuses on precision farming.

Dr. Shariff was the recipient of the recognition of the DUO Denmark Fellowship award etc. He is a Chartered Agricultural Engineer, Fellow, and Life Member of the Malaysian Society of Agricultural Engineers, member of the Institution of Agricultural Engineers, American Society of Agricultural and Biological Engineers.

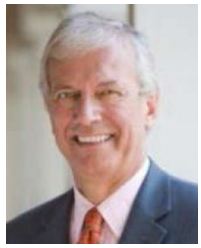

John R. Townshend received the B.Sc. and Ph.D. degrees in geography from University College London, London, U.K.

He is an Emeritus Professor with the Department of Geographical Sciences, University of Maryland, College Park, USA. He has held faculty positions with Tanzania's University of Dar es Salaam, the University of Reading, U.K., Clark University, Worcester (USA).

Dr. Townshend was the recipient of an NRC Senior Fellowship for research at NASA's Goddard Space Flight Center, the William T. Pecora Award for Outstanding Leadership in Advancing Global Remote Sensing in 2005, and an Honorary Fellowship from the United Kingdom's Remote Sensing and Photogrammetry Society. He is a Fellow of the American Association for the Advancement of Science and the Royal Geographical Society. He has held Honorary Professorships at the University of Wuhan, the Chinese Academy of Agricultural Sciences, and the Center for Earth Observations and Digital Earth of the Chinese Academy of Sciences.